Influence of external vibration on tether chain in ligand-receptor binding

Bin Xue and Wei Wang

Citation: J. Chem. Phys. **122**, 194912 (2005); doi: 10.1063/1.1900727
View online: http://dx.doi.org/10.1063/1.1900727
View Table of Contents: http://jcp.aip.org/resource/1/JCPSA6/v122/i19
Published by the American Institute of Physics.

Influence of external vibration on tether chain in ligand-receptor binding

Bin Xue and Wei Wang[a)]
National Solid State Microstructure Laboratory, Institute of Biophysics, Nanjing University, Nanjing 210093, People's Republic of China and Department of Physics, Nanjing University, Nanjing 210093, People's Republic of China

(Received 3 February 2005; accepted 10 March 2005; published online 19 May 2005)

The tethered ligand-receptor binding is an important biological phenomenon. The conformation of tether chain greatly affects the binding process. By using molecular dynamics, the influence of environmental vibration on the conformation of the tether chain is studied. The phase diagram shows that the radius of gyration of the tether chain becomes large when there is vibration due to the vibrational disturbance. However, when the vibration frequency is high enough, the average value of radius of gyration will reduce. Under high frequency vibration, the chain has an inerratic variation on its radius of gyration. These properties provide the frequency modulation on the dimension of the chain. The scaling relation proves the dimension of chain increases faster under low frequency vibration. There are also weak resonance and stochastic-resonance-like behaviors in the chain system. These behaviors probably have biological importance. © *2005 American Institute of Physics*. [DOI: 10.1063/1.1900727]

I. INTRODUCTION

The ligand-receptor binding is a very common biological phenomenon and plays an important role in integrin signaling, cell adhesion, cell spreading and migration, cell death, and many other biological processes.[1–3] The binding of ligand with receptor has characteristics other than the normal interaction between two trivial biomolecules. The first is the specificity which only allows specific ligand to have strong binding interaction with particular receptor. The second is the relatively small force range of the binding interaction. Since the force range is in the order of several angstroms, which is about one order of magnitude less than the dimension of ligand or receptor. Besides, the local dimension of the surfaces on which both of the ligand and receptor are bound, is typically two orders larger than that of the force range.

In many cases, the ligands are bound on the surface through flexible tether chains while the receptors are directly fixed on the surface.[4] Under these circumstances, due to the specificity and short-range property of ligand-receptor binding, the tether chain will apparently have prominent influence on the binding behavior, and will further affect the whole biological process. These results have already been validated by various experiments. In the experiment of choosing poly(ethylene glycol) as the tether chain and biotin-streptavidin as the ligand-receptor system, respectively, it has been demonstrated that the ligand-receptor binding is decided by the rare events of the R_g distribution of the tether chains, i.e., the conformation of large radius of gyration.[4,5] The ligand on the large R_g tether chain will bind to the adjacent receptor first. Under the circumstance that the separation trend is weak, more and more ligand-receptor pairs could be formed in succession. Thus, two apart cells or cell and extracellular matrix on which the ligands or receptors are attached, respectively, can be pulled together or have biological interactions.

Based on the understanding on the importance of tether chain, many researches have been proceeded on what factors will affect the conformation of the chain. It has been found that the grafted tether chains may vary as a function of their density on the surface.[6–8] At low density, the conformation of tether chain shows a mushroom regime which indicates the chain is more globulelike. While under high density, the chain is in a brush regime in which the conformation of the chain is more extended and the radius of gyration of the chain is apparently larger. Besides the impact of density, it shall be more interesting to investigate the influence on tether chain of the cellular environment. This influence may be raised by the movement of the cell, the flow of body fluid, or the external factors. It is also reported that the clustering of ligands will facilitate the signaling process which is the outcome of ligand-receptor binding.[9] Among all kinds of external disturbance, shear flow is one kind of extensively studied situation, in respect of its obvious linkage to the real physical situations. Usually, the flow can be simplified as simple shear flow,[10] channel flow,[11] oscillatory shear flow,[12] random three-dimensional flow,[13] and so on. In the case of shear flow, the flow has important influence on the conformation of one-end-fixed chain. Both experimental[14] and theoretical[10] studies prove that the distribution of the extension of the chain is decided by the shear rate. However, due to the complexity of the extracellular environment, it is also interesting to adopt other kinds of disturbances during the study. Especially, it has been reported that the external mechanical vibration may facilitate the osteogenesis.[15,16] And up to our knowledge, there is no computational simulation analysis on the rare events distribution of the tether chain under external disturbance. The understanding of this issue is beneficial not only to the theoretical researches, but also to

[a)]Author to whom correspondence should be addressed. Electronic mail: wangwei@nju.edu.cn

the engineering applications. Here in this paper, we simplify the external environmental disturbance as a periodic oscillation. In this circumstance, the movement of tether chain will be driven by the external periodic oscillation. The Langevin dynamics is applied to simulate the movement of the chain system. The result shows that the external vibration indeed has important influence on the radius of gyration and may provide a mechanism of frequency modulation.

This paper is arranged as follows. In Sec. II, the model and methods are introduced. In Sec. III, the results and discussions are presented. Then in Sec. IV, a summary is given.

II. MODEL AND METHOD

The tether chain is modeled by a coarse-grained flexible homopolymer chain, which is composed of monomers connected by bonds. One terminus of the homopolymer chain is fixed on a surface. In many experiments, the tether chain is made of poly(ethylene glycol), which is also known as poly-(ethylene oxide), and is water soluble.[17,18] Thus, the monomers on the chain are supposed to be hydrophilic. Meanwhile, the surface represents the outer layer of the lipid bilayer of cells. Hence, the surface is also considered to be hydrophilic.

The consecutive monomers on the homopolymer chain have a bond potential,[19]

$$U_{\text{bond}} = k_1(r_{j,j+1} - d_0)^2 + k_2(r_{j,j+1} - d_0)^4, \tag{1}$$

where $k_1=1$ and $k_2=100$, and $d_0=3.8$ Å is the bond length.

The interaction between nonconsecutive monomers is Leonard-Jones (LJ) potential,

$$U_{\text{LJ}} = \varepsilon\left[\left(\frac{\sigma}{r_{ij}}\right)^{12} - 2\left(\frac{\sigma}{r_{ij}}\right)^{6}\right]. \tag{2}$$

Here, ε is the strength and is set to be 1, $\sigma=6.5$ Å is potential constant.

Since both the surface and monomer are considered to be hydrophilic, a LJ-like potential is applied between the monomers on the homopolymer chain and the surface. The form of the interaction is obtained from the integration over the surface by assuming that the interaction between monomer and the surface molecule is also LJ potential,[20]

$$U_s = \rho\varepsilon_s\left[\frac{1}{5}\left(\frac{\sigma}{h_i}\right)^{10} - \frac{1}{2}\left(\frac{\sigma}{h_i}\right)^{4}\right], \tag{3}$$

where ρ is the density of hydrophilic molecules on the surface, and h_i is the distance from the monomer to the surface, ε_s is the strength (constants have been absorbed in). In this paper, the surface is supposed to have a constant density of $\rho=1.2$.

The force induced by the external vibration is

$$F = F_0\cos(2\pi\omega t), \tag{4}$$

where F_0 is the magnitude of the force, ω is the vibrational frequence, and t is the time. In the simulations, ω varies from 20 Hz to 10^7 Hz which is in the range of both audio and ultrasonic frequency. There are two reasons for choosing such a frequency range. First, most of the possible vibrations that happened in a living body are within such a range. Second, the ultrasonic vibration has many applications. The force is set on the direction perpendicular to the surface.

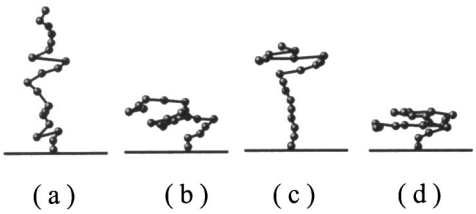

FIG. 1. The schematic graph of the tether chain under various vibration conditions. (a) The initial extended conformation of the chain. (b) and (c) are two states of the chain during the simulation at time steps of 8×10^7 and 7×10^6, respectively, under the external vibration of $f=1.5$ and $\omega=200$ kHz. (d) The equilibrium state of the chain without external vibration.

The Verlet Leap-frog algorithm is used to proceed to the Langevin equation.[21] The friction coefficient in the Langevin equation is $\xi=0.05$. The initial conformation of the tether chain is chosen as an extended random coil obtained at high temperature. The integration time step h in the simulation is set to be $h=0.005\tau$, where $\tau=a\sqrt{m/\varepsilon}$ is the character time of the system with m the mass of each bead. In reduced unit, we set $m=1$, $\varepsilon=1$, $a=1$, thus $\tau=1$. In most of the cases, the simulation lasts for 10^9 steps. For the purpose of analyzing specific trajectories, the simulation time is prolonged to 2×10^9 steps. The real time that corresponds to this process is around 15 μs which can roughly match to many biologically interested time scales. Trajectories up to 100 are simulated to get the ensemble average.

In Fig. 1, a schematic drawing for the influence of external vibration on the tether chain and the comparison with equilibrium state of the same chain without external vibration is presented. The bottom lines indicate the hydrophilic surface. The initial conformation of the chain is rather extended as given in Fig. 1(a). The external vibration may both squeeze the chain or enlarge the chain as shown in Figs. 1(b) and 1(c). In Fig. 1(d), it can be found that the equilibrium state of the chain is the most collapsed. Due to the weak repulsion from the hydrophilic surface, this state is slightly distorted from a random globule.

III. RESULTS AND DISCUSSIONS

Figure 2 presents the change of radius of gyration as a function of vibration frequency under various vibration forces. From this figure, it is clear that generally the bigger the vibration force, the larger the radius of gyration is, and the higher the vibration frequency, the smaller the radius of gyration is. In addition, when the vibration frequency is less than 10^3 Hz, the average radius of gyration shows a saturated value for each case. This indicates that within the simulation time scale, the frequency adjustment has no influence on the conformation of the chain. When the vibration frequency is beyond 10^5 Hz, the average radius of gyration under each vibration force shows a symptotic property. At the low limit of vibration frequency, when the vibration forces are $f=0.1$, 0.5, 1.0, 1.2, 1.3, 1.4, and 1.5, respectively, the values of radius of gyration are 6.15, 6.39, 7.23, 8.07, 11.44, 14.06, and 15.7 Å accordingly. While at the high limit of vibration frequency, the corresponding values of radius of gyration at

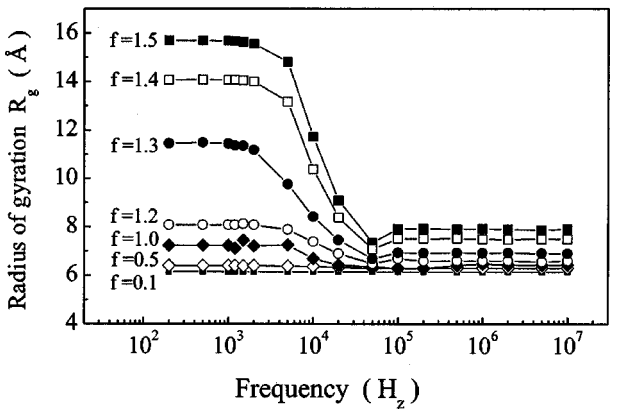

FIG. 2. The variation of R_g as a function of vibration frequency under different forces. The frequency is cutoff at 10^7 Hz which includes both audio and ultrasonic vibrations.

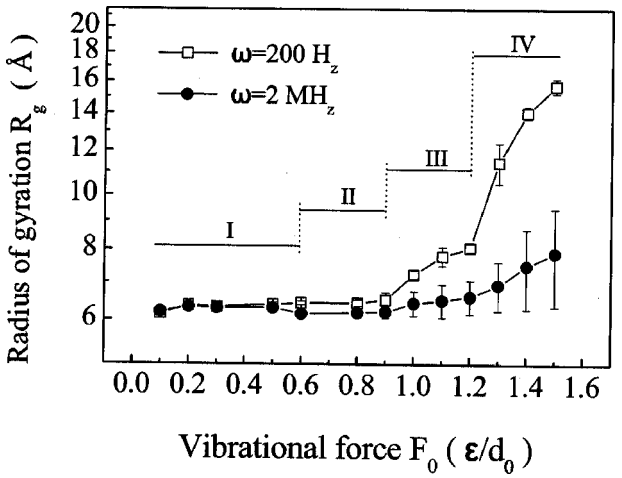

FIG. 3. The influence on R_g of the vibration force at two specific frequencies. The open square is for $\omega=200$ Hz while the filled circle is for $\omega=2\times10^6$ Hz. Apparently, the full scope of available force is divided into four ranges.

the same vibration forces are 6.15, 6.3, 6.28, 6.59, 6.92, 7.51, and 7.93 Å, respectively. Apparently, the differences of radius of gyration between various forces at high frequency limit are smaller than that at the side of low frequency. In the frequency range of 2×10^3 Hz$<\omega<5\times10^4$ Hz, there is a sharp decrease of the radius of gyration, especially under the cases where the vibration force $f>1.0$. The decreasing rates for $f=1.0$, 1.2, 1.3, 1.4, and 1.5 are -0.02, -0.03, -0.09, -0.14, and -0.17 (Å/kHz), accordingly. The negative sign indicates that the radius of gyration decreases with the increasing of vibration frequency. Obviously, the chain system has a frequency sensitivity at this frequency range. It will be demonstrated in the following that this frequency sensitivity may probably be a time effect. In the cases of $f\leqslant0.5$, the radius of gyration has no detectable changes when the vibration frequency is scanned over the whole spectrum (200 Hz$<\omega<10^7$ Hz). Hence, when the external disturbance becomes weak, the frequency sensitivity of the chain system disappears. This property is quite similar to the stochastic resonance in the nonlinear dynamic system.[22] Another interesting phenomenon in this figure is the overall minimum of radius of gyration at $\omega\sim5\times10^4$ Hz. This minimum is more distinguishable when the vibration force is bigger than $f\sim1.2$. This minimum may correspond to the ultrasound absorption observed in experiments.[7]

The results in Fig. 2 state that the influence of vibration force on radius of gyration is very intricate. Even at both limits of low and high frequency ($\omega<10^3$ Hz and $\omega>2\times10^5$ Hz), the variation of R_g along with f is irregular. Let alone in the middle range of 2×10^3 Hz$<\omega<5\times10^4$ Hz where R_g changes quickly with the magnitude of force. Nevertheless, it is necessary to analyze the influence of the magnitude of vibration force on the radius of gyration at least at the two extremes. The relation between R_g and vibration force at two specific frequencies, which are $\omega=200$ Hz and $\omega=2\times10^6$ Hz, is presented in Fig. 3. It is obvious that the influence of vibration force on R_g can be roughly divided into four stages. When the vibration force is less than 0.5, the influence of both vibration force and frequency on the radius of gyration is very limited. This conclusion is inferred by the observation that under these two frequencies, the values of R_g are coincident and do not alter with the enhancement of force. When $0.5<f<0.9$, the value of R_g does not change with the increasing of force, but the values of R_g at two different vibration frequencies are apparently distinguishable, i.e., the high frequency vibration reduces the average value of R_g. The value of R_g at $\omega=200$ Hz is 6.5 Å, and decreases to 6.2 Å at $\omega=2\times10^6$ Hz. When the force is enhanced to $f=1.2$, the value of R_g at low frequency increases faster than that at high frequency. The increasing rate for $\omega=200$ Hz is about 5.2 [in the unit of Å/(ϵ/d_0)], while at $\omega=2\times10^6$ Hz, the increasing rate is 1.3. Moreover, the standard deviation of R_g under high frequency begins to increase greater than that of low frequency. This indicates that the conformation of chain during the simulation under high frequency vibration may have prominent changes. When the vibration force is further increased to $f=1.5$, the value of R_g at $\omega=200$ Hz increases strongly, the increasing rate is 25.4, while the increasing rate for $\omega=2\times10^6$ Hz is 4.3. And the standard deviation in this case grows further to around 1.5 Å. In brief, the radius of gyration will generally increase with the enhancing of vibration force, and the increment of R_g is smaller at high vibration frequencies than at low frequencies. However, when the frequency is high, in the force range of $0.5<f<0.9$, the radius of gyration has a local minimum compared with that in the force ranges of $f<0.5$ and $f>0.9$. This is also a resemblance to the stochastic resonance.

The reason why the radius of gyration at bigger forces is much larger than that under smaller forces, especially when the vibration frequency is low, is that the initial direction of the force during the simulation is set to be in favor of producing loose conformations. In Fig. 4, the influence on the radius of gyration of the initial direction of force is presented. The different initial directions of the force are realized by changing the initial phase of the vibration. The chain length in Fig. 4 is also $N=20$. Obviously, in the case of high frequency which is $\omega=200$ kHz, when $f=1.0$, R_g varies between 6.25 and 6.5 Å; while $f=1.2$, the value of R_g is between 6.5 and 6.7 Å. This indicates that under the influence of high frequency vibration, the initial phase will not affect the average value of radius of gyration. However, when the

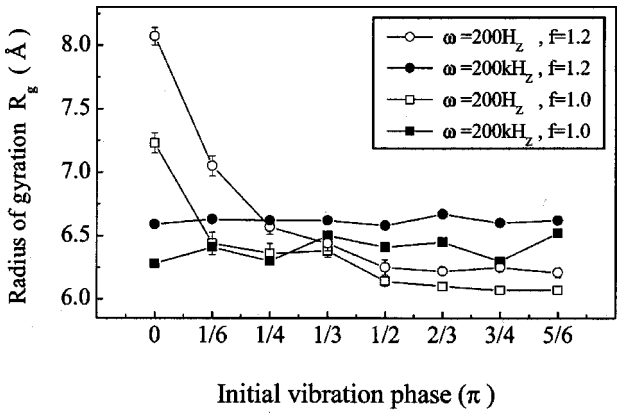

FIG. 4. The influence on R_g of the initial phase of the vibration at two different forces and two various frequencies. The open circle and square are under frequency of $\omega=200$ Hz, the filled circle and square are at $\omega=200$ kHz. The open and filled circles are with a force of $f=1.2$, while the open and filled squares are $f=1.0$.

vibration frequency is $\omega=200$ Hz, as shown by the open circles and open squares in the graph, the initial phase has apparent influence on the radius of gyration. In the case of $f=1.0$, when the initial phases are $\phi=0$, $1/6\pi$, $1/4\pi$, $1/3\pi$, $1/2\pi$, $2/3\pi$, $3/4\pi$, and $5/6\pi$, the equilibrium values of R_g are 7.2, 6.4, 6.3, 6.4, 6.2, 6.1, 6.1, and 6.1 Å, accordingly. And the corresponding values of R_g at various initial phases under $f=1.2$ are 8.1, 7.1, 6.6, 6.4, 6.3, 6.2, 6.3, and 6.2 Å, respectively. Hence, the values of R_g decrease about 30% and 20% for $f=1.2$ and $f=1.0$, accordingly, when the initial phase is reversed. It can also be found that when the initial phase is changed from $\phi=0$ to $\phi=1/6\pi$, the values of R_g reduce 15% and 12% for $f=1.2$ and $f=1.0$, respectively. These results come from the facts that the vibration force is changed as a cosine function. When the initial phase increases from $\phi=0$ to $\phi=1/6\pi$, the magnitude of the vibration force will decrease about 15% of its initial value. It can also be expected that when the force is large, the decreasing of absolute value of R_g at the first $1/6\pi$ of initial phase shall be bigger than that at other similar ranges of initial phase. When the initial phase is over $1/2\pi$, the direction of the vibration force is in the reverse direction which is to squeeze the chain. Hence, the radius of gyration of the chain is expected to decrease further. However, this effect is counteracted by the excluded volume of the chain. Another issue that shall be noticed is that when the initial phase is bigger than $1/2\pi$, the radius of gyration under low frequency is smaller than that at high frequency. While in the cases of $\phi<1/2\pi$, the situations are basically on the contrary. This is also due to the reversal change of the direction of vibration force.

From the above discussions, it is apparent that the vibration periodicity will affect the average value of the radius of gyration. Hence it shall be meaningful to investigate the variation of R_g during the whole simulation process. The low frequency situation is shown in Fig. 5(a). The vibration frequency in Fig. 5(a) is $\omega=200$ Hz. The dashed line is the magnitude of vibration force in half a cycle. The solid line at the left side of the graph is the trace of R_g in a trajectory of total 10^9 time steps. The inset is the magnified presentation

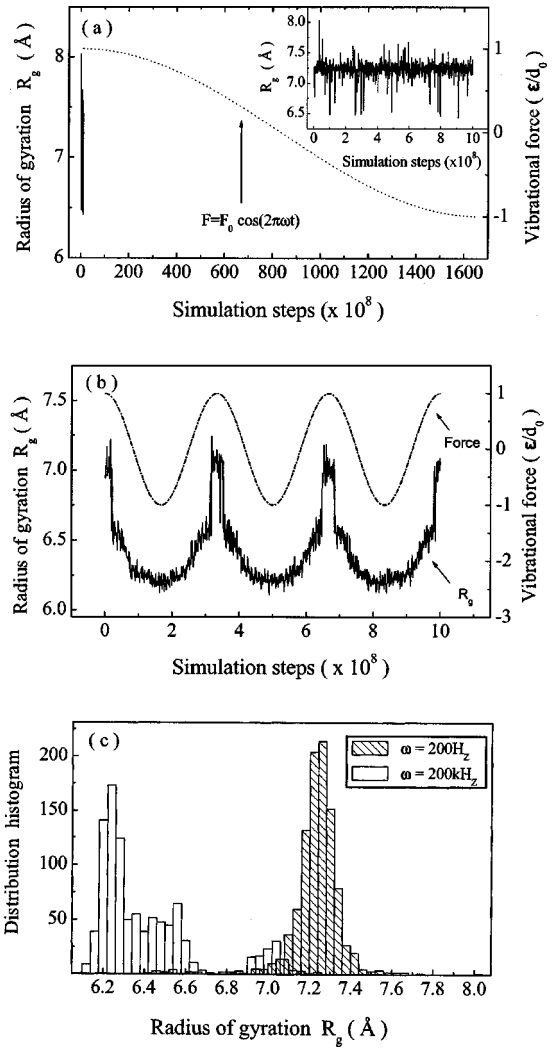

FIG. 5. The distribution of R_g at two frequencies $\omega=200$ Hz and $\omega=200$ kHz. (a) The time evolution of R_g at $\omega=200$ Hz, the dashed line is the vibration force in half a cycle. The inset is a magnified picture for the solid line at the left side. (b) The variation of R_g with time at $\omega=200$ kHz. (c) The histogram distributions of R_g at above two frequencies.

of the above trajectory. It is clear from the dashed line that half of one cycle is equivalent to 1.65×10^{11} time steps, and are in the real time of 2.5 ms. Thus, the first $1/6\pi$ of one circle is about 0.4 ms. Within such a time interval, the force will be changed by about 15% at most in the magnitude. It is also apparent in the inset that in the whole simulation trajectory, the value of R_g fluctuates around 7.25 Å. In most cases, R_g is between 7.0 and 7.5 Å. Only in some rare cases, the value of R_g may reach to 8.0 Å as the maximum, and may decrease to 6.5 Å as the minimum. The fluctuation of R_g indicates that in the simulation, the conformation of the chain has random variations. The high frequency situation is presented in Fig. 5(b). The vibration frequency in Fig. 5(b) is $\omega=200$ kHz. The dashed line is the change of force in 10^9 time steps. The solid line is for R_g in the same time period. Different from what is shown in Fig. 5(a), R_g in Fig. 5(b) shows a synchronous oscillation with the vibration force. Further analysis indicates that with the decreasing of the magnitude of the vibration force, this synchronous phenomenon becomes weak. However, detailed comparison between

the force and R_g shows that the variation of R_g does not exactly follow the pace of f. The first disaccord is the different time intervals staying at the maximal value and the minimal value of R_g. It can be seen from the figure that the time interval at $R_g \sim 7.0$ Å is about 2×10^7 time steps in one cycle, while the time residing at $R_g \sim 6.25$ Å is around 2×10^8 time steps. Meanwhile, the distribution of force at two extremes are symmetrical. The second disagreement is the sharp droppings of R_g from large values to small ones, and the corresponding abrupt ascents at symmetrical positions. At the time of $t\sim 2\times10^7$, the value of R_g drops very quickly from 7.0 to 6.6 Å in about 10^6 time steps. And at $t\sim 3.15\times10^7$ steps, R_g increases from 6.6 to 7.0 Å in around 10^6 time steps. These two hops in one cycle bring on an anomalous distribution of R_g which only prefers the high and low values of R_g, not the intermediates. In the meantime, the force decreases rather smoothly. This may indicate that there is a critical value for the vibration force, under this value, the intrinsic stability of the chain system dominates; beyond this value, the chain becomes adjustable. The high frequency behavior of R_g actually may provide more content in the frequency modulation of R_g.

By comparing Figs. 5(a) and 5(b), it can be seen that the distribution of R_g at low frequency is centralized with only one most probable value; while at high frequency, the distribution of R_g is separated into at least two regions. This result is shown in Fig. 5(c). It is clear that when $\omega=200$ kHz, the distribution of R_g has apparently two preferred regions, one is at $R_g \sim 6.2$ Å with an extension to $R_g=6.6$ Å, another one is located at $R_g \sim 7.0$ Å. The first peak of distribution at 6.2 Å corresponds to the three minima in Fig. 5(b). The flat distribution between 6.4 and 6.6 Å is for the sampling between the sharp droppings and the minima in Fig. 5(b). And the small peak at 7.0 Å represents the specific distribution when the force is around the maximum value. While for $\omega=200$ Hz, there is only one peak sited at $R_g \sim 7.2$ Å. This is also in accordance with what is shown in Fig. 5(a). From this figure, it can be easily concluded that when there is no external disturbance, the distribution of R_g is Gaussian-like. However, when the external vibration is introduced into the system, the distribution will be greatly distorted. It can also be stated that in the case of high frequency, the distribution at larger value of R_g is narrower than that at smaller values of R_g. Hence, the chain can be considered to have good cooperativity at the larger value of R_g. Although the morphology of distribution for R_g varies for different combinations of frequency and force, it is still possible to describe the distribution properties by simple methods. We can calculate the average values of the lowest 60% and the highest 5% of R_g in the simulation to give an explicit description on the distribution of R_g. These two average values are denoted by $R_{g,L}$ and $R_{g,H}$, respectively. The bigger the value of $R_{g,L}$, the looser the average conformation is. The smaller the value of $R_{g,H}$, the more compact the chain is.

From the above discussions, it is clear that both the vibration force and the vibration frequency will affect the distribution of radius of gyration of the chain. By adopting the quantities of $R_{g,L}$ and $R_{g,H}$, it is possible to construct the phase diagram of the influence of both vibration force and

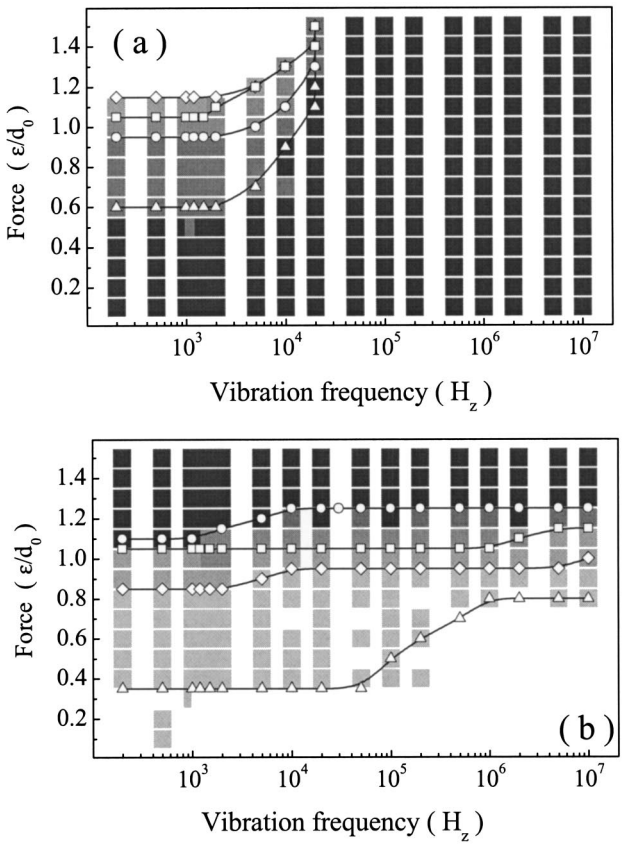

FIG. 6. Two phase diagrams for the distribution of R_g as a function of both vibration force and frequency. (a) The distribution of average value of the lowest 60% of R_g in the simulation. The open triangle, open circle, open square, and open diamond indicate the board lines of 5%, 10%, 20%, and 30% above the native value of R_g, respectively. (b) The distribution of average value of the highest 5% of R_g in the simulation. The open triangle, open diamond, open square, and open circle denote values of 5%, 15%, 25%, and 35% above the value of R_g^N, respectively.

frequency. These combined influence of vibration force and vibration frequency is shown in Figs. 6(a) and 6(b). In Fig. 6(a), the darkness of each large square indicates the average value of the lowest 60% of all values of R_g in the simulation. Since this average value of R_g is only an average over samples, it can also be interpreted as the time staying in the compact conformations during the simulation. The color of gray means the average value of R_g is small, while the white indicates a large R_g. The open triangles are the board line where the averaged R_g is 5% higher than the native value R_g^N. Similarly, the open circles, the open squares, and the open diamonds are side lines of 10%, 20%, and 30% higher than R_g^N, accordingly. All the side lines are horizontal at the low limit of vibration frequency. When $\omega>2\times10^3$ Hz, these lines will go up with the frequency. Finally, the four board lines converge into one when $f>1.4$ and $\omega>2\times10^4$ Hz. When the statistics are over the lowest 80% of all the values of R_g in the simulation, the results are resemblant to the current one. This statistical result provides directly the observation on the probability of the chain in its compact conformation. Generally, the chain intends to stay in a compact conformation under higher frequencies, while at higher forces the chain is apparently looser. It can be seen from this figure that when the vibration force is weaker than $f=0.6$, the

chain is always in the compact conformation at least most of the time. When the vibration frequency is higher than 2×10^4 Hz, the chain also has a high probability in a compact conformation no matter the magnitude of the force.

However, because the chain has large conformation fluctuation during the simulation, it is not enough to know only the probability in compact states. Furthermore, many biological processes are initiated by the rare events of the distribution. Thus, it shall be interesting to present the average value of R_g which is in the largest conformation during the simulation. This result is shown in Fig. 6(b). The large squares are the average values of the top 5% of R_g in the simulation. The dark squares denote large average value, while the lighter ones are for small average R_g. The open triangles at the bottom indicate a side line of 5% higher than the native radius of gyration R_g^N. Correspondingly, the open diamonds, the open squares, and the open circles are for the board lines of 15%, 25%, and 35% higher than the native radius of gyration R_g^N, respectively. It is clear that the open-triangle line is horizontal when the vibration frequency is less than $\omega\sim5\times10^4$ Hz. Afterwards, with the increasing of frequency to $\omega\sim10^6$ Hz, this line increases almost logarithmically from $f=0.35$ to $f=0.8$. Further increasing the frequency, this line is again horizontal. From this line, it can be concluded that when the vibration force is less than $f=0.35$, the vibration frequency has no obvious impact on $R_{g,H}$. In addition, with the increasing of frequency, $R_{g,H}$ is becoming smaller than that at the same force but low frequency. And finally, when the frequency is high enough ($\omega>10^6$ Hz), lifting the frequency will not reduce the value of $R_{g,H}$. The open-diamond line shows the similar trend. When $\omega<2\times10^3$ Hz, the line is aclinic at $f=0.85$. In the range of 2×10^3 Hz$<\omega<10^4$ Hz, the line goes up from $f=0.85$ to $f=0.95$. For frequencies over $\omega=10^4$ Hz, the line keeps the position at $f=0.95$ with an exception at $\omega=10^7$ Hz. The open-square line is also horizontal until the frequency is higher than 10^6 Hz which is the same as in the open-triangle line. The last one is the open-circle line. This line is aclinic at frequencies less than 10^3 Hz or larger than 10^4 Hz. Within the range between the above two frequencies, the line increases logarithmically with the frequency. The general picture shown in this figure is very interesting, i.e., with adjusting the force and the frequency, the average maximal value of $R_{g,H}$ can be controlled.

It is also interesting to study the scaling behaviors of the chain under various vibration frequencies. The results are shown in Fig. 7. When there is vibration in the system, the vibration force is chosen as $f=1.0$. The scaling relation of Flory chain is calculated from the Flory theory and is placed here as a reference. For Flory chain, the scaling relation is $R_g\sim N^{0.6}$, where N is the length of the chain. Apparently, the approximate scaling relation for the chain under no vibration is similar to that of Flory chain. However, the critical index in this case is only about 0.42, which means $R_g\sim N^{0.42}$. This originates from the weak interaction between membrane plate and the monomers on the chain. For the case of $\omega=200$ Hz, when the chain length is less than 40, there is no obvious scaling relation between R_g and chain length. However, the radius of gyration increases very fast with the chain length in an exponential style. When the chain length is longer than 40, it is found that $R_g\sim N^{1.75}$. In the high frequency case of $\omega=200$ kHz, there seems to be two scaling relations depending on the chain length. For short chains with $N<30$, $R_g\sim N^{0.85}$. When the chain length is longer than 30, the critical index is 1.55. These results are not surprising. When there is vibration, longer chains will be distorted much more than the short chains no matter if the vibration frequency is high or low.

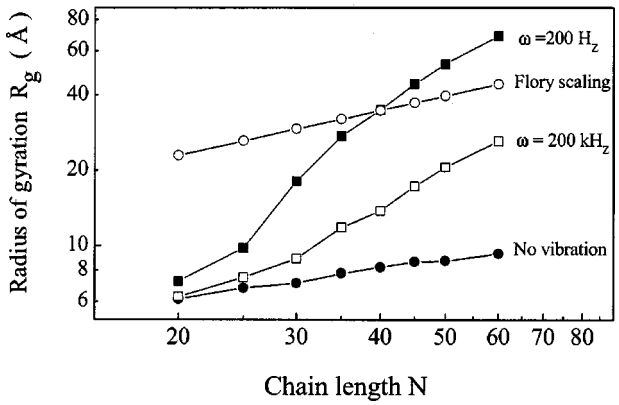

FIG. 7. The scaling relations under various conditions. The open circle is calculated from the Flory theory for the random chain. The filled circle is for the chain without vibration but tethered on the membrane. The filled square and open square are under vibration of $\omega=200$ Hz and $\omega=200$ kHz, accordingly.

It has been demonstrated in Figs. 5(a) and 5(b) that with the increasing of vibration force, the value of R_g may jump between several specific values. However, in Fig. 5(b), the distribution at small value of R_g is much more and broader, whereas the distribution at large value of R_g is very concentrated. This analysis may lead to an expectation that there seems to be a specific frequency at which the distribution of R_g is more regular. Figure 8(a) is the change of radius of gyration in one specific simulation trajectory. The chain length is $N=20$, the force is $f=1.0$, the vibration frequency is $\omega=1.2\times10^3$ Hz. The change of radius of gyration is shown by the solid line at the left side of the graph. The inset is also the trajectory cut off at 10^9 time steps. The dashed line is the variation of vibration force in half of one periodicity. It can be seen that during the simulation, due to the low vibration frequency, the force is unable to change greatly in such a short time period. However, the radius of gyration still has big fluctuations. The inset clearly shows the fluctuations. The radius of gyration of the chain has two major distributions, one is around $R_g=7.05$ Å, another one is about $R_g=8.2$ Å. R_g is either around 20% or about 33% bigger than the native value R_g^N. The transition from one value of R_g to another is very abrupt. Each time, the real time period that R_g is at a smaller value is less than 1 μs, then R_g recovers to the bigger value. In most times of the simulation process (~15 μs), the tether chain has a bigger value of R_g. Clearly, the chain has a "two-state" behavior, which is supposed to be correlated with the resonance or the chain system. Moreover, since the difference between these two values of R_g is less than one order of magnitude, the resonance can only be regarded as a weak one.

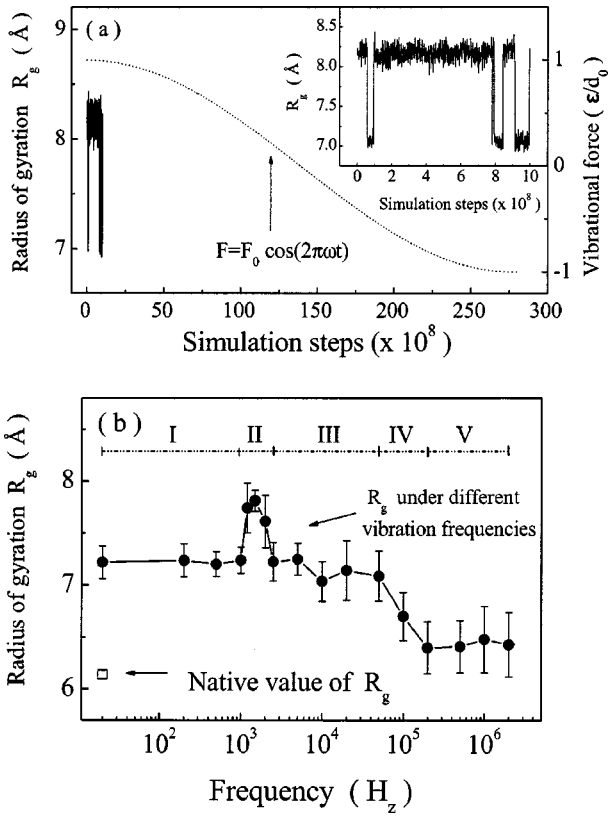

FIG. 8. The specific frequency property at $f=1.0$. (a) The change of R_g in one trajectory at $\omega=1200$ Hz, the dashed line is the vibration force in half a cycle. The inset is the trajectory cutoff at 10^9 time steps. (b) The relation of R_g with frequency. The frequency spectrum is divided into five regions.

Since $\omega=1.2\times10^3$ is a specific frequency for the chain system, it shall be interesting to analyze the value of R_g in the whole frequency spectrum. Actually, it has been shown in Fig. 2 that when $f=1.0$ and $\omega=1.2\times10^3$, there is a relatively large fluctuation of R_g. This plot is again shown in Fig. 8(b). The open square sign at the left-bottom corner is the R_g at native state, which is acquired by simulated annealing, while the curve linked by the filled circles denotes the average R_g under different external vibrational frequencies. It is clear that when there is external vibration, R_g is always bigger than that without the vibration. The variation of R_g along with the frequency can be divided into five parts. Region I is the low frequency region ($20\ \text{Hz}<\omega<1000$ Hz). The increment of R_g than without vibration is around 20%. And in this region, the influence of vibrational frequency on R_g is robust. In region II, where frequency scope is $1000\ \text{Hz}<\omega<2500$ Hz, R_g shows a maximal increasing of 33% compared with that without vibration. The frequency ranges of region I and region II are actually very narrow, which are only about 1000 Hz. At higher frequencies of region III ($2500\ \text{Hz}<\omega<50$ kHz), R_g shows the robust again and is in the same magnitude as in the first region. In region IV which is the highest for audio wave ($50\ \text{kHz}<\omega<200$ kHz), R_g will decrease with raising the frequency. The frequency boundary for region III and region IV is $\omega=50$ kHz. Vibration of this frequency may complete one cycle of vibration in a simulation time of 10^9 steps. Then in region V which is the scope of ultrasonic wave ($\omega>200$ kHz), R_g will not change with the frequency. However, the average R_g in this range is only 5% higher than that without the vibration.

IV. SUMMARY

In this paper, the influence of external vibration on tethered chain in the ligand-receptor binding process is studied. This research is focused on a short time scale of about 15 microsecond. The long time behaviors of the tethered chain will be discussed in the future. However, since many biological processes are proceeded within such a time period, this limitation on the time scale is still of practical meaning. The system of the model is composed of the tethered chain and the membrane on which the chain is bound. Both of the tethered chain and the surface of membrane are supposed to be hydrophilic.

Through the molecular dynamics simulation under various vibration forces and frequencies, it is testified that generally the larger the vibration force, the looser the conformation of the chain, and the higher the vibration frequency, the more compact the chain is. Under low frequency, R_g increases faster with the strengthening of vibration force than that under higher frequency. While at high frequency, the enlarging of R_g with the force is relatively slow. The initial phase of the vibration has an important impact on the radius of gyration in the low frequency case. However, when the frequency is high enough, there is almost no influence of vibration on R_g.

The trajectory analysis shows that when the frequency is low, the distribution of R_g is around one specific value. As a comparison, under high frequency, the value of R_g varies roughly in the same pace as the vibration force does. The distribution of R_g is separated into at least two peaks. However, the distributions at various values of R_g are unsymmetrical. In addition, the transition between high and low values of R_g is abrupt. It is also found that under one specific vibration frequency ($\omega\sim1.2$ kHz), there is a weak resonance in the chain system. The phase diagrams of the distribution of R_g provides more direct illustration on the frequency properties of the chain. There are some key frequencies under which the system shows important transitions. These results indicate that it is possible to realize the frequency control over the radius of gyration of the tether chain and probably have engineering applications.

ACKNOWLEDGMENTS

This work was supported by the National Natural Science Foundation of China (Grant Nos. 90103031, 10474041, 90403120, and 10021001), and the Nonlinear project of NSM (Grant No. G2000077300).

[1] F. G. Giancotti and E. Ruoslahti, Science **285**, 1028 (1999).
[2] L. B. Smilenov, A. Mikhailov, R. J. Pelham, Jr., E. E. Marcantonio, and G. G. Gundersen, Science **286**, 1172 (1999).
[3] C. S. Chen, M. Mrksich, S. Huang, G. M. Whitesides, and D. E. Ingber, Science **276**, 1425 (1997).
[4] J. Y. Wong, T. L. Kuhl, J. N. Israelachvili, N. Mullah, and S. Zalipsky, Science **275**, 820 (1997).
[5] C. Jeppesen, J. Y. Wong, T. L. Kuhl, J. N. Israelachvili, N. Mullah, S. Zalipsky, and C. M. Marques, Science **293**, 465 (2001).

[6]T. L. Kuhl, J. Majewski, J. Y. Wong, S. Steinberg, D. E. Leckband, J. N. Israelachvili, and G. S. Smith, Biophys. J. **75**, 2352 (1998).
[7]O. Tirosh, Y. Barenholz, J. Katzhendler, and A. Priev, Biophys. J. **74**, 1371 (1998).
[8]M. L. Wagner and L. K. Tamm, Biophys. J. **79**, 1400 (2000).
[9]D. J. Irvine, K. A. Hue, A. M. Mayes, and L. G. Griffith, Biophys. J. **82**, 120 (2002).
[10]T. Haliloglu, I. Bahar, and B. Erman, J. Chem. Phys. **105**, 2919 (1996).
[11]Y. Radzyner and D. C. Rapaport, Phys. Rev. E **57**, 5687 (1998).
[12]R. Mäkinen, J. Ruokolainen, O. Ikkala, K. De Moel, G. ten Brinke, W. De Odorico, and M. Stamm, Macromolecules **33**, 3441 (2000).
[13]A. Groisman and V. Steinberg, Phys. Rev. Lett. **86**, 934 (2001).
[14]D. E. Smith, H. P. Babcock, and S. Chu, Science **283**, 1724 (1999).
[15]C. Rubin, G. Xu, and S. Judex, FASEB J. **15**, 2225 (2001).
[16]J. M. Lamothe and R. F. Zernicke, J. Appl. Phys. **96**, 1788 (2004).
[17]T. L. Kuhl, D. E. Leckband, D. D. Lasic, and J. N. Israelachvili, Biophys. J. **66**, 1479 (1994).
[18]P. L. Hansen, J. A. Cohen, R. Podgornik, and V. A. Parsegian, Biophys. J. **84**, 350 (2003).
[19]C. Clementi, A. Maritan, and J. R. Banavar, Phys. Rev. Lett. **81**, 3287 (1998).
[20]G. S. Grest, J. Chem. Phys. **105**, 5532 (1996).
[21]M. P. Allen and D. J. Tildesley, *Computer Simulation of Liquids* (Clarendon, Oxford, 1989).
[22]P. Hanggi, P. Jung, and F. Marchesoni, Rev. Mod. Phys. **70**, 223 (1998).